Available online at www.sciencedirect.com
SCIENCE DIRECT®
Nuclear Instruments and Methods in Physics Research B 242 (2006) 55–60
NIM B
Beam Interactions with Materials & Atoms
www.elsevier.com/locate/nimb

A study on the electronic stopping of protons in soft biological matter

D. Emfietzoglou [a,f], A. Pathak [b,c,*], G. Papamichael [d], K. Kostarelos [e], S. Dhamodaran [b], N. Sathish [b], M. Moscovitch [f]

[a] Department of Medical Physics, University of Ioannina Medical School, Ioannina 451 10, Greece
[b] School of Physics, University of Hyderabad, Central University (P.O.), Hyderabad 500 046, Andhra Pradesh, India
[c] Departmento de Fisica, UAM Iztapalapa, Apartado Postal 55 534, 09340 Mexico, DF, Mexico
[d] Department of Mechanical Engineering, National Technical University of Athens, Athens 157 10, Greece
[e] School of Pharmacy, University of London, London WC1N 1AX, UK
[f] Department of Radiation Medicine, Georgetown University Medical Center, Washington, DC 20007, USA

Available online 21 September 2005

Abstract

The electronic stopping of protons in liquid water has been investigated by means of the dielectric function properties. Based on a modified Drude dielectric model, an accurate analytic parametrization of the two sets of available optical data for liquid water has been accomplished. The resultant optical loss functions predict an I-value of 80–85 eV. Extension to finite momentum is included by means of simple dispersion algorithms. The influence of different dielectric function approximations and of the higher-order Z_1-corrections to the stopping power (SP) of liquid water for protons in the 50–1000 keV range is explored. This includes the Bragg peak which, among other things, is of great interest in radiation dosimetry and in predicting radiation damage. The model calculations are within 10–12% of ICRU values with the larger deviations being observed below the SP maximum. The higher-order Z_1-corrections, associated with the Barkas and Bloch effects, contribute minimally (<2%) down to the Bragg peak region (~100 keV). At the low end examined (50–100 keV) the Z_1^4-term increases more rapidly than the Z_1^3-term and their net contribution increases.

1. Introduction

The electronic stopping of protons in soft biological matter is of importance in various medical [1] and space [2] applications where energetic light-ions are involved. Liquid water represents a standard approximation of soft tissue because of its high abundance in biological cells (70–80%). Moreover, its electronic excitation spectrum is similar to most organic compounds while its dissociation products include very reactive free-radicals which represent a ubiquitous mechanism of radiation induced biological damage [3].

Knowledge of the electronic stopping power (SP) of liquid water for protons down to the Bragg peak is of importance in radiation dosimetry and in predicting radiation damage. Bethe's theory represents the standard framework for calculating the SP above its maximum [4–6]. At energies near the Bragg peak, though, Bethe's SP is less accurate due to the limitations of the first Born approximation (proportional to Z_1^2) and of the dipole approximation in the mean excitation and ionization energy; the I-value [7,8]. The latter is the important material-dependent quantity in Bethe's SP formula associated with the quantized electronic structure of the target. In the non-relativistic range, it represents an important source of uncertainty because it depends on the absorption spectrum spanning from threshold up to the X-ray region where experimental information is difficult to obtain. Furthermore, at the Bragg peak region the dipole approximation – essentially a high-energy approximation – is of decreasing validity due to the reduced contribution of inner-shell electrons. Shell-corrections are meant to correct

* Corresponding author. Address: School of Physics, University of Hyderabad, Central University (P.O.), Hyderabad 500 046, Andhra Pradesh, India. Tel.: +91 40 23010181/23134316; fax: +91 40 23010181/23010227.
E-mail address: appsp@uohyd.ernet.in (A. Pathak).

0168-583X/$ - see front matter © 2005 Elsevier B.V. All rights reserved.
doi:10.1016/j.nimb.2005.08.001

for this deficiency but their theoretical evaluation is difficult to perform for realistic targets.

Finally, in the Bragg peak the strength of the interaction cannot be accounted for within first-order perturbation theory. Higher-order corrections, proportional to Z_1^3 and Z_1^4, need to be introduced to account (at least partially) for the Barkas and Bloch effects, respectively [8]. The above methodology becomes problematic below the Bragg peak where the SP becomes proportional to the projectile velocity; this energy range is not examined here.

A successful methodology for heavy ion stopping including the above effects is the binary theory of Sigmund [9]. The potential of this theory to describe light ion stopping has been also shown [10]. An alternative quantal approach based on the first Born approximation proceeds by means of the dielectric function for the material [11]. Inner-shell effects associated with Bethe's shell-corrections are automatically included in the calculations through the variation of the dielectric function over the energy–momentum plane; thus, explicitly accounting for terms beyond the dipole approximation. Due to its importance, work on the dielectric function of liquid water with application to charged particle transport has been recently revived [12–18]. Extending our earlier work we present here new SP calculations for protons down to the Bragg peak in liquid water. The effect of different dielectric function approximations and of the higher-order Z_1-corrections on proton SP values is examined.

2. Methodology

The calculation of the stopping power of condensed matter within first-order dielectric theory, $SP^{(1)}$, begins with the expression [11]:

$$-\frac{dE^{(1)}}{dx}=\frac{Z_1^2}{\pi\alpha_0 T}\int \hbar\omega\, d(\hbar\omega)\int \frac{1}{k}\,\mathrm{Im}\left[\frac{-1}{\varepsilon(k,\omega)}\right]dk, \tag{1}$$

where $\alpha_0=\hbar/me^2$ is the Bohr radius, Z_1 is the projectile's charge, $T=mV^2/2$ with m the electron rest mass and V the projectile velocity, $\varepsilon(k,\omega)$ is the complex dielectric response function and $\hbar\omega$ and $\hbar k$ are the energy and momentum transfer, respectively. For the present energy range, the value $Z_1=1$ for protons is assumed. The $\mathrm{Im}(-1/\varepsilon)=\mathrm{Im}(\varepsilon)/|\varepsilon|^2$ is the key material property called the loss function. The $\mathrm{Im}(\varepsilon^{(j)})=\varepsilon_2^{(j)}$ is associated with the absorption of a photon inducing the jth electronic transition, whereas a deviation of $|\varepsilon|^2=\varepsilon_1^2+\varepsilon_2^2$ from unity signals the influence of the condensed phase in particle–matter interaction. The following approximation has been adopted:

$$\mathrm{Im}\left[\frac{-1}{\varepsilon(k,\omega)}\right]\cong\sum_{\text{valence}}\frac{\mathrm{Im}[\varepsilon^{\mathrm{v}}(k,\omega)]}{|\varepsilon^{\mathrm{v}}(k,\omega)|^2}+\mathrm{Im}\left[\varepsilon^{\mathrm{K}}(k,\omega)\right], \tag{2}$$

where

$$\mathrm{Im}\left[\varepsilon^{\mathrm{K}}(k,\omega)\right]=\frac{\pi}{2}\frac{\omega_p^2}{Z}\frac{df(k,\omega)}{\omega\, d(\omega)}. \tag{3}$$

In Eqs. (2) and (3) "v" denotes valence transitions, "K" denotes K-shell ionization, $\omega_p=\sqrt{4\pi Ne^2/m}$ with N the electronic density, Z is the atomic number and $df(k,\omega)/d\omega$ is the atomic generalized-oscillator-strength. In the present work, the loss function of the valence shells is established by a semi-empirical procedure which has found much use [19]. For the valence shells, the two sets of available data [20,21] for the optical limit of $\mathrm{Im}(\varepsilon)$ of liquid water were analytically represented by a superposition of normal (for the continuum) and derivative (for the discrete) Drude functions appropriately modified to account for multi-shell electrons:

$$\varepsilon_2^{\mathrm{v}}(0,\omega)=(\hbar\omega_p)^2\sum_j^{\text{ioniz}}\left\{\frac{A_j\Gamma_j(\hbar\omega)}{[B_j^2-(\hbar\omega)^2]^2+(\Gamma_j\hbar\omega)^2}\right\}+(\hbar\omega_p)^2\sum_j^{\text{excit}}\left\{\frac{2A_j\Gamma_j^3(\hbar\omega)^3}{[(B_j^2-(\hbar\omega)^2)^2+(\Gamma_j\hbar\omega)^2]^2}\right\}. \tag{4}$$

For the K-shell, we use photoionization data for oxygen to describe the atomic optical-oscillator-strength:

$$\frac{df^K(0,\omega)}{d(\hbar\omega)}=(4\pi^2\alpha\alpha_0^2R)^{-1}\sigma_{\mathrm{ph}}^{\mathrm{K}}, \tag{5}$$

where α is the fine structure constant and σ_{ph}^K the oxygen's K-shell photoionization cross-section. By means of Eq. (3) $\varepsilon_2^{\mathrm{K}}(0,\omega)$ is then readily obtained. In the Drude representation of the optical data, the parameters A_j, B_j and Γ_j are associated with the height, position and width, respectively, of each transition peak in the spectrum. Consistent with current experimental evidence [22], plasmon excitation is neglected and only single-electron transitions are considered. Nevertheless, the use of experimental optical data accounts, by default, for possible collective effects in the liquid phase. The consistency of the analytic representation of the optical data was secured by satisfying the f-sum-rule:

$$S^{\mathrm{K}}=\frac{2}{\pi}\int_0^\infty\frac{\omega}{\omega_p^2}\varepsilon_2^{\mathrm{K}}(0,\omega)\,d\omega=0.178, \tag{6}$$

$$S^{\mathrm{v}}=\frac{2}{\pi}\int_0^\infty\frac{\omega}{\omega_p^2}\varepsilon_2^{\mathrm{v}}(0,\omega)\,d\omega=1-S^{\mathrm{K}}. \tag{7}$$

The value of 0.178 in Eq. (6) is known from the literature [23]. From Eq. (4), the $\mathrm{Re}(\varepsilon)$ may be obtained by Kramers–Kronig analysis, or, because of the form of the Drude functions, analytically. The following expression is obtained:

$$\varepsilon_1^{\mathrm{v}}(0,\omega)=1+(\hbar\omega_p)^2\sum_j^{\text{ioniz}}\left\{\frac{A_j[B_j^2-(\hbar\omega)^2]}{[B_j^2-(\hbar\omega)^2]^2+(\Gamma_j\hbar\omega)^2}\right\}+(\hbar\omega_p)^2\sum_j^{\text{excit}}\left\{\frac{A_j[B_j^2-(\hbar\omega)^2][(B_j^2-(\hbar\omega)^2)^2+3(\Gamma_j\hbar\omega)^2]}{[(B_j^2-(\hbar\omega)^2)^2+(\Gamma_j\hbar\omega)^2]^2}\right\}. \tag{8}$$

The extension of the optical loss function ($k=0$) to the momentum space ($k>0$) is accomplished by means of a

dispersion relation. The extended-Drude model and the δ-oscillator models are most appropriate for describing the dispersion of interband transitions and have, therefore, been extensively applied to liquid water and other organic compounds; see [17] and references therein. Recently, Penn's statistical model with a single-pole approximation to Lindhard's function has been applied to biological materials and shown to be equivalent to the plasmon-like δ-oscillator dispersion [24]. In the extended-Drude model of Ritchie and co-workers [25], the binding shell energies B_j are dispersed in the sense of the impulse approximation:

$$B_j(k) = B_j(0) + (\hbar k)^2/2m, \tag{9}$$

where $B_j(0) \equiv B_j$, whereas the discrete transitions are damped but not dispersed using an empirically derived generalized-oscillator-strength for H_2O. In the δ-oscillator model of Ashley [26], the momentum-dependence of the loss function is given by:

$$\mathrm{Im}\left[\frac{-1}{\varepsilon(k,\omega)}\right] = \frac{1}{\omega}\int_0^\infty \omega' \mathrm{Im}\left[\frac{-1}{\varepsilon(0,\omega')}\right]\delta(\omega-\omega'(k))\,\mathrm{d}\omega', \tag{10}$$

where a plasmon-like quadratic dispersion formula for $\omega'(k)$ is adopted:

$$h\omega'(k) = \hbar\omega'(0) + (\hbar k)^2/2m. \tag{11}$$

On the other hand, in the δ-oscillator model of Liljequist [27], the optical limit and a delta-like Bethe-ridge are used avoiding any particular dispersion formula. The momentum-dependence of the loss function is obtained by:

$$\mathrm{Im}\left[\frac{-1}{\varepsilon(k,\omega)}\right] = \frac{1}{\omega}\int_0^\infty \omega' \mathrm{Im}\left[\frac{-1}{\varepsilon(0,\omega')}\right]F_\delta(\omega';k,\omega)\,\mathrm{d}\omega', \tag{12}$$

where a two-mode δ-oscillator is used:

$$F_\delta(\omega';k,\omega) = \delta(\omega-\omega')\Theta(\hbar\omega'-Q(k)) + \delta(\hbar\omega-Q(k))\Theta(Q(k)-\hbar\omega'), \tag{13}$$

where $Q(k) = (\hbar k)^2/2m$ is the free-electron recoil energy. It may be easily shown that all the above schemes exhibit the correct asymptotic behavior at $k = 0$ and $k \gg 0$.

At low energies corrections to the first Born approximation are required. Typically, higher-order corrections proportional to Z_1^3, and Z_1^4 are introduced to account for the Barkas and Bloch effects, respectively. In the present work, we follow Ashley's [28] second-order Z_1^3-correction term for the Barkas effect:

$$-\frac{\mathrm{d}E^{\mathrm{Corr}}_{\mathrm{Barkas}}}{\mathrm{d}x} = \frac{Z_1^3}{\pi\alpha_0 T}\int \hbar\omega\,\mathrm{Im}\left[\frac{-1}{\varepsilon(0,\omega)}\right]L_1(\omega;\xi)\,\mathrm{d}(\hbar\omega), \tag{14}$$

where the function $L_1(\omega;\xi)$ contains the free parameter ξ associated with the cut-off distance of glancing collisions. We examine here two choices of ξ as discussed in [28]. For the Z_1^4-correction term of the Bloch effect we use Bichsel's formula [29]:

$$-\frac{\mathrm{d}E^{\mathrm{Corr}}_{\mathrm{Bloch}}}{\mathrm{d}x} = \frac{(\hbar\omega_p)^2}{2\alpha_0 T}\{-y^2[1.202 - y^2 \times (1.042 - 0.855y^2 + 0.343y^4)]\}, \tag{15}$$

where $y = Z_1\alpha/\beta$.

In Bethe's theory, the $SP^{(1)}$ of Eq. (1) is solved analytically using the *f*-sum-rule and the dipole approximation. The end result is the following simple formula:

$$-\frac{\mathrm{d}E_{\mathrm{Bethe}}}{\mathrm{d}x} = \frac{(\hbar\omega_p)^2}{2\alpha_0 T}Z_1^2\ln\left(\frac{4T}{I}\right). \tag{16}$$

The mean excitation and ionization energy of the material (the *I*-value) may be expressed in terms of the optical loss function as follows:

$$\ln(I) = \frac{\int_0^\infty \omega\ln(\hbar\omega)\,\mathrm{Im}\left[\frac{-1}{\varepsilon(0,\omega)}\right]\mathrm{d}\omega}{\int_0^\infty \omega\,\mathrm{Im}\left[\frac{-1}{\varepsilon(0,\omega)}\right]\mathrm{d}\omega}. \tag{17}$$

Note that from the difference of Eq. (16) and the full solution of Eq. (1) the shell-corrections of Bethe's SP formula may be obtained.

3. Results and discussion

In Fig. 1, our optical ($k = 0$) loss function model is compared against the two available sets of data for liquid water; the reflectance measurements of [20] and the more recent Compton scattering data of [21]. Despite its simplicity, the model provides an accurate analytic representation of the data, especially at the important region around the 20 eV peak where a broad absorption maximum is observed. Interestingly, the two sets of data differ by about a factor of 1.7 at the peak region. As it has been discussed in [21] the new data, being closer to that of amorphous ice, might be closer to reality. Despite the unrealistic asymptotic behaviour of the Drude functions the sum-rules were satisfied to within 1%. Furthermore, our optical loss functions predict an *I*-value between 80 and 85 eV in agreement with both the recent experimental value 79.75 + 0.50 eV [30] and a model prediction 81.8 eV [10], The recommended ICRU *I*-value is 75 eV [31].

In Fig. 2(a) and (b), our model loss function is plotted for different values of the wavenumber *k* (panel a) and frequency ω (panel b) using the extended-Drude and δ-oscillator dispersion models. The impulse-approximation used in the extended-Drude model and the plasmon-like quadratic dispersion in the δ-oscillator model provide a somewhat similar dependence of the loss function on momentum. In contrast, the two-mode δ-oscillator model, which uses only the optical limit and a δ-like Bethe-ridge, is increasingly inaccurate at low energy and momentum values.

In Fig. 3, we present calculated SP values using our two different optical loss functions obtained from the

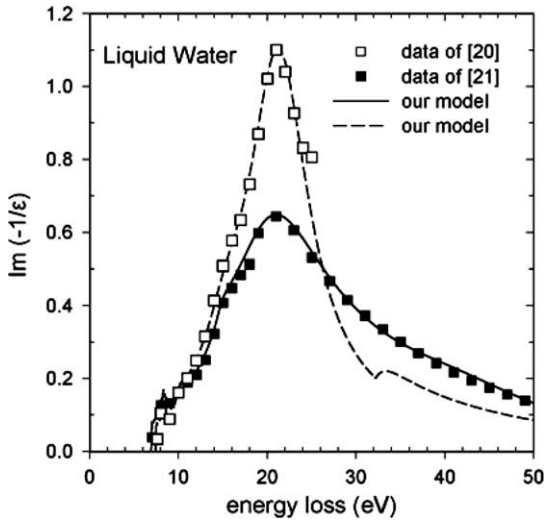

Fig. 1. The optical loss function of liquid water as obtained by our empirically-adjusted modified Drude model and compared against the experimental data; open symbols: the old reflectance measurements of [20]; filled-symbols: the recent Compton scattering measurements of [21].

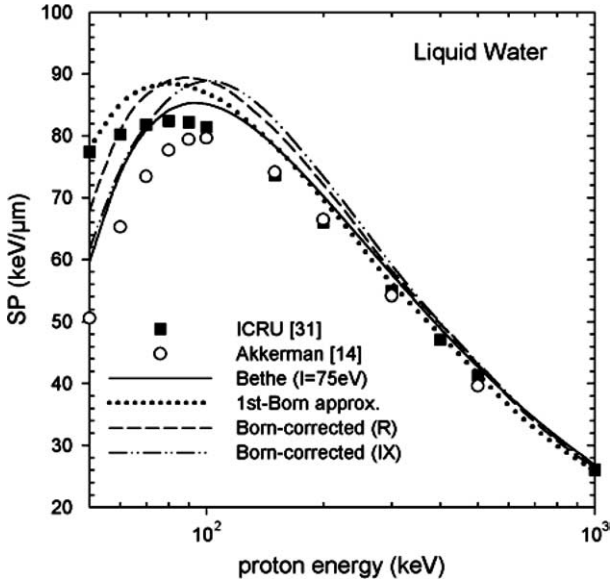

Fig. 3. The electronic stopping power of liquid water for protons in the 50–1000 keV range. Our calculations include the first Born approximation and the Born-corrected formulae using our optical-data models (R: the reflectance-based; IX: the Compton-based) and the extended-Drude dispersion, Bethe's formula with $I = 75$ eV. For comparison also included are the dielectric calculations of [14] and the ICRU values [31].

reflectance (R) and Compton scattering (IX) data dispersed in accordance with the extended-Drude model and corrected for the Barkas and Bloch effects. First Born calculations (i.e. uncorrected) and results based on Bethe's SP formula with $I = 75$ eV are also presented. For comparison, we include the ICRU values [31] and the recent calculations of Akkerman and Akkerman [14]. The latter uses a different optical loss function parametrization of the reflectance data and the plasmon-like δ-oscillator dispersion. Differences between the various SP curves increase gradually below about 500 keV and become largest at the Bragg peak ($\sim$100 keV) and below. The calculations are within 10–12% from ICRU values. This, however, is about the level of the uncertainty of the ICRU values at the region of the maximum. It is of interest to note that (i) our uncorrected calculations are slightly closer to ICRU than the calculations including the higher-order Z_1-corrections and (ii) the calculations using the more recent Compton data exhibit a somewhat larger deviation from ICRU than the ones using the old reflectance data. In agreement with Akkerman all model calculations fall more sharply below the

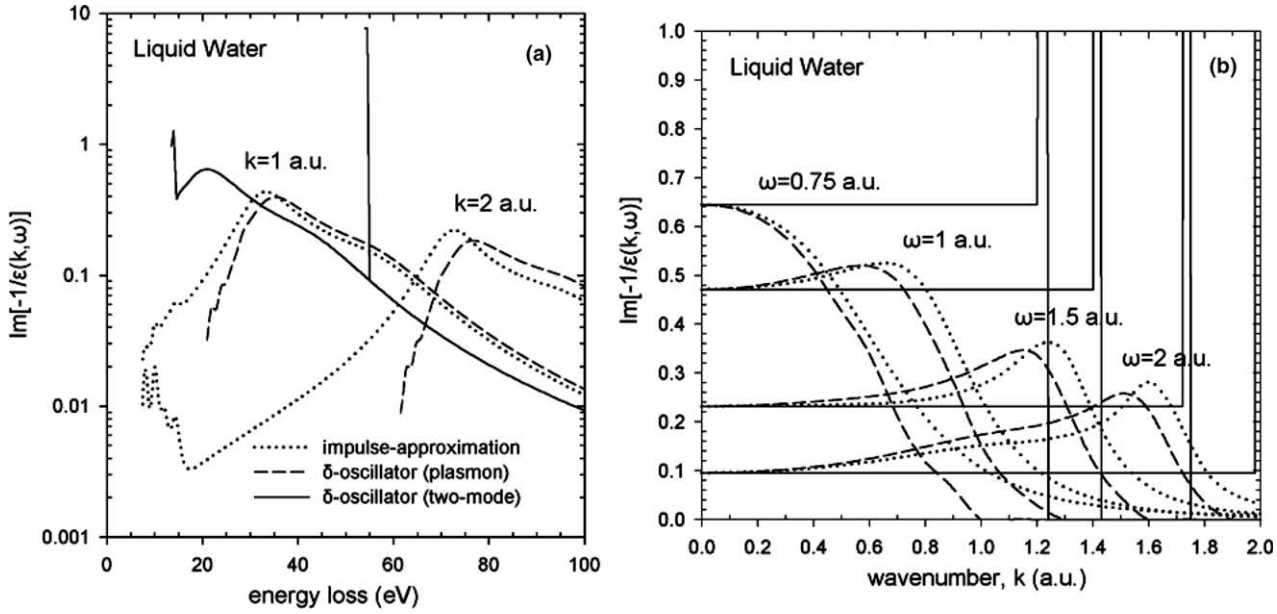

Fig. 2. The loss function of liquid water for: (a) two different values of momentum transfer $\hbar k$ and (b) for various values of energy transfer $\hbar\omega$. Our optical model derived from the Compton data [21] has been used for all calculations presented.

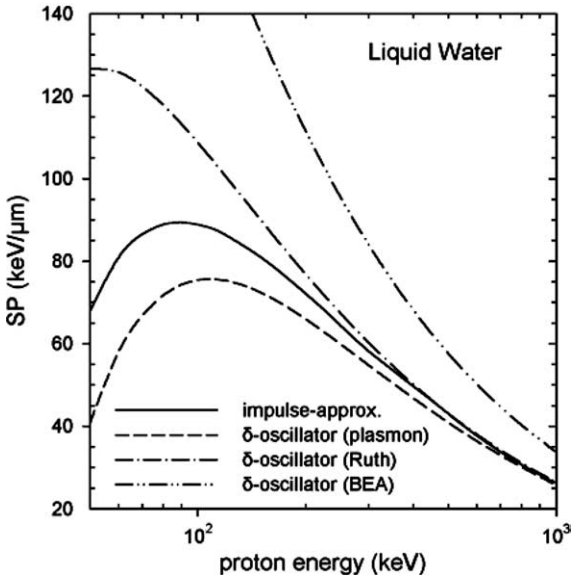

Fig. 4. The electronic stopping power of liquid water for protons calculated by various dispersion models. Our optical model derived from the Compton data [21] has been used for all the calculations presented.

maximum than the ICRU values. This is the region, however, where the validity of the models is questionable and Lindhard's theory (or its modifications), where the SP is proportional to the projectile velocity, should be used. Though not shown, the use of Lindhard's impact parameter value in the Z_1^3-term provides results that deviate significantly at the Bragg peak region. Also, it was found that the use of a simple binary encounter formula (BEA) for the K-shell, instead of an atomic generalized-oscillator-strength, would affect the total SP by less than 10%.

In Fig. 4, the influence of the various dispersion algorithms in the SP is presented. The Compton-based optical loss function has been used for all calculations depicted. Calculations with the two-mode δ-oscillator model have been performed using both a Rutherford and a BEA hard-collision component. Both alternatives deviate substantially at low energies and, therefore, their use should be restricted to the MeV region. The impulse approximation and the plasmon-like dispersion differ by about 20% at the Bragg peak; the latter being about 10% below the ICRU values [31].

In Fig. 5, the contribution of the various Z_1-terms is evaluated. Despite the rapid increase in magnitude of both the Barkas (Z_1^3) and Bloch (Z_1^4) terms below a few hundred keV, because of their opposite signs their net contribution to the total SP remains less than 2% down to 80 keV. At the low energy end examined (50–80 keV) the Bloch term becomes larger than the Barkas term and, therefore, their net contribution becomes significant.

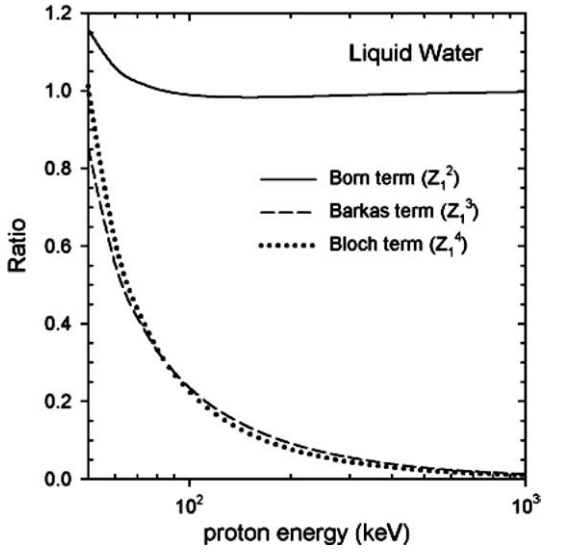

Fig. 5. The ratio of each Z_1-term to the Z_1-corrected stopping power.

4. Conclusion

The energy and momentum dependent dielectric function of liquid water constructed from optical data and dispersion algorithms has been used to investigate the electronic stopping power of protons from the MeV down to the Bragg peak region. Using a reasonable assumption about dispersion, calculations are within 10–12% of ICRU values. Below the Bragg peak maximum ($\sim$100 keV) all model calculations fall more sharply than the ICRU predictions. Higher-order Z_1-corrections appear to contribute minimally (<2%) down to the Bragg peak. At even lower energies the Bloch correction (Z_1^4-term) increases more rapidly than the Barkas correction (Z_1^3-term) and their net contribution may become significant.

Acknowledgements

Research sponsored by the US Department of Energy under contract DE-AC05-960R22464 (NN-22 Program) with UT Battelle and by the University of Loannina Committee of Research Grant no. 62/1405.

References

[1] A. Brahme, Int. J. Radiat. Oncol. Biol. Phys. 58 (2004) 603.
[2] H. Nikjoo, S. Uehara, I.G. Khvostunov, F.A. Cucinotta, W.E. Wilson, D.T. Goodhead, Phys. Med. 17 (2001) 38.
[3] H. Nikjoo, P. O'Neill, W.E. Wilson, D.T. Goodhead, Radiat. Res. 156 (2001) 577.
[4] H. Bethe, Z. Physik. 76 (1932) 293.
[5] U. Fano, Ann. Rev. Nucl. Sci. 13 (1963) 1.
[6] P. Sigmund, Nucl. Instr. and Meth. B 135 (1998) 1.
[7] G. Basbas, Nucl. Instr. and Meth. B 4 (1984) 227.
[8] P. Sigmund, Nucl. Instr. and Meth. B 85 (1994) 541.
[9] P. Sigmund, Stopping of Heavy Ions: A Theoretical Approach, Springer Tracts in Modern Physics, Vol. 204, Springer Verlag, Germany, 2004.
[10] P. Sigmund, A. Schinner, Nucl. Instr. and Meth. B 193 (2002) 49.
[11] R.H. Ricthie, Nucl. Instr. and Meth. 198 (1982) 81.
[12] M. Dingfelder, D. Hantke, M. Inokuti, H.G. Paretzke, Radiat. Phys. Chem. 53 (1998) 1.
[13] M. Dingfelder, M. Inokuti, Radiat. Environ. Biophys. 38 (1999) 93.
[14] A. Akkerman, E. Akkerman, J. Appl. Phys. 86 (1999) 5809.

[15] M. Dingfelder, M. Inokuti, H.G. Paretzke, Radiat. Phys. Chem. 59 (2000) 255.
[16] A. Akkerman, A. Breskin, R. Chechik, Y. Lifshitz, Radiat. Phys. Chem. 61 (2001) 333.
[17] D. Emfietzoglou, M. Moscovitch, Nucl. Instr. and Meth. B 193 (2002) 71.
[18] D. Emfietzoglou, M. Moscovitch, A. Pathak, Nucl. Instr. and Meth. B 212 (2003) 101.
[19] C.J. Powel, A. Jablonski, J. Phys. Chem. Ref. Data 28 (1999) 19.
[20] J.M. Heller, R.N. Hamm, R.D. Birkhoff, L.R. Painter, J. Chem. Phys. 60 (1974) 3483.
[21] H. Hayashi, N. Watanabe, Y. Udagawa, C.-C. Kao, Proc. Natl. Acad. Sci. USA 97 (2000) 6264.
[22] C.D. Wilson, C.A. Dukes, A. Baragiola, Phys. Rev. B 63 (2001) 121101.
[23] M. Inokuti, J.L. Dehmer, T. Baer, H.D. Hanson, Phys. Rev. A 23 (1981) 95.
[24] Z. Tan, Y. Xia, M. Zhao, X. Liu, F. Li, B. Huang, Y. Li, Nucl. Instr. and Meth. B 222 (2004) 27.
[25] R.H. Ritchie, R.N. Hamm, J.E. Turner, H.A. Wright, W.E. Bolch, in: W.A. Glass, M.N. Varma (Eds.), Physical and Chemical Mechanisms in Molecular Radiation Biology, Plenum, New York, 1991, p. 99.
[26] J.C. Ashley, J. Appl. Phys. 69 (1991) 674.
[27] D. Liljequist, J. Phys. D: Appl. Phys. 16 (1983) 1567.
[28] J.C. Ashley, J. Phys.: Condens. Matter. 3 (1991) 2741.
[29] H. Bichsel, Phys. Rev. A 41 (1990) 3642.
[30] H. Bichsel, T. Hiraoka, Nucl. Instr. and Meth. B 66 (1992) 345.
[31] ICRU Report 49, International Commission on Radiation Units and Measurements, Bethesda, MD, 1984.